



# Interconnection and Damping Assignment Passivity-Based Control Design Under Loss of Actuator Effectiveness

Zhong Liu<sup>1,2,3</sup> · Didier Theilliol<sup>4</sup> · Liying Yang<sup>1,2</sup> · Yuqing He<sup>1,2</sup> · Jianda Han<sup>1,2,5,6</sup>

Received: 24 April 2019 / Accepted: 3 February 2020 / Published online: 14 March 2020  
© Springer Nature B.V. 2020

## Abstract

Due to the convenience in applications, interconnection and damping assignment passivity-based control (IDA-PBC) is applied widely to reformulate the nonlinear robust control as the total energy shaping. However, only few researches focus on the fault-tolerant control (FTC) method based on IDA-PBC, which limits its applications under actuator faults. To break this limitation, this paper improves the IDA-PBC with fault-tolerant ability, and the main contributions are to propose high-gain and adaptive IDA-PBC methods under loss of actuator effectiveness. The simulation and experiment results with a rotorcraft unmanned aerial vehicle (RUAV) are presented to illustrate the control effectiveness of the improved IDA-PBC methods.

**Keywords** IDA-PBC · Loss of actuator effectiveness · Passive FTC · RUAV

## 1 Introduction

Passivity-based control (PBC) is a powerful technique to design nonlinear and robust controllers for physical systems modelled by Euler-Lagrange (EL) equations [1]. Classical PBC stabilizes physical systems by “shaping” only potential energy, and assigns a dissipative closed-loop energy function equal to the difference between the original energy of controlled plant and the energy from designed controller [2]. To shape the total energy of controlled plant, [2] and [3] propose interconnection and damping assignment passivity-based control (IDA-PBC), which constructs the closed-loop energy function by desired subsystem interconnections and damping [3]. Superior to classical PBC, IDA-PBC relies on a more general system description — port-controlled Hamiltonian (PCH) model rather than the EL equation. Due to the convenience for nonlinear controller design and inherent robustness against unmodeled dynamics, IDA-PBC has been applied widely for the control of manipulator [4], rotorcraft unmanned aerial vehicle (RUAV) [5], RUAV slung load system [6], and electrical system [7].

To ensure stability or acceptable control performance of controlled plant under sensor faults or actuator faults, nonlinear passive and active fault-tolerant control (FTC) methods have been researched for a long time [8] based on sliding mode control [9–11], backstepping control [12–15], and linear parameter-varying (LPV) control [16–18]. Reference [19] further carries out the comparative study between passive and active approaches to provide an objective assessment for them. However, according to the authors’ knowledge, only a few of researches focus on the fault-tolerance based on classical passivity or IDA-PBC. For example, [20] applies passivity theory to ensure the stability of nonlinear systems under loss of actuator effectiveness, and [21] introduces integral action into IDA-PBC to deal with matched and constant disturbances. Above lack of attention separates passivity from stability analysis under different faults.

Aiming at extending IDA-PBC into the control under loss of actuator effectiveness, this paper improves the IDA-PBC with fault-tolerant ability, and two passive FTC methods are proposed without the fault detection and identification (FDI) strategy. Due to the loss of actuator effectiveness reduces control performance obviously, high-gain IDA-PBC is proposed first to improve nominal controller performance based on the lower bound of actuator faults, and  $\mathcal{L}_2$  stability of closed-loop system could be ensured via passivity. Then, to avoid above dependence on the lower bound of actuator faults, adaptive IDA-PBC is considered further inspired

✉ Didier Theilliol  
didier.theilliol@univ-lorraine.fr

by [13] and [14]. The asymptotic stability of closed-loop system could be ensured with an adaptive control law, and the actuator saturation is taken into account by an auxiliary state vector. To alleviate the dramatic fluctuations of the adaptive control inputs in stable case, a modified version of this adaptive method is proposed immediately.

The main contributions of this paper are to propose high-gain and adaptive IDA-PBC methods for the control under loss of actuator effectiveness, and to extend IDA-PBC technique into FTC for actuator faults, which is seldom considered in existing references. Compared with some other passive FTC methods for loss of actuator effectiveness [9, 10, 12, 14, 15, 18], the proposed methods inherit the advantages of IDA-PBC, and are robust against unmodeled dynamics, which provide the convenience for real applications. To illustrate the effectiveness of the proposed methods, some simulation results are displayed with the rotational dynamics of a hexarotor unmanned aerial vehicle (UAV). The hovering flight experiments are carried out further with high-gain IDA-PBC for rolling motion control under loss of actuator effectiveness. Due to the varying battery voltage and flight maneuver, the actuator dynamics of the real platform is uncertain. To solve this problem, unscented Kalman filter (UKF) [22] is applied offline with regular flight data to estimate and determine the upper and lower bounds of uncertain actuator dynamics. Then these uncertain actuator dynamics could be transformed into the actuator fault formulation and dealt with by high-gain IDA-PBC.

The remaining parts of this paper are organized as follows: Section 2 introduces some useful knowledge about passivity and general IDA-PBC technique; Section 3 formulates the FTC problem under loss of actuator effectiveness and actuator saturation first, and presents the proposed high-gain and adaptive IDA-PBC methods further; some simulation and experiment results are displayed in Section 4 to illustrate the effectiveness of the proposed methods; section V ends the whole paper with conclusions.

In following contents, let  $\|\bullet\|$  mean Euclidean norm,  $\nabla$  represent gradient,  $\lambda_{\min}([\bullet])$  and  $\lambda_{\max}([\bullet])$  mean minimum and maximum eigenvalues of matrix  $[\bullet]$ ,  $I_n$  be identity matrix with  $n$ -dimension,  $\text{diag}(\bullet)$  mean diagonal matrix,  $\text{Mu}([\bullet]) = [\bullet]^T \cdot [\bullet]$ ,  $(\lambda_{\max} \cdot \text{Mu})([\bullet]) = \lambda_{\max}(\text{Mu}([\bullet]))$ , and  $\text{sign}(\bullet)$  represent sign operator.

## 2 Preliminary

### 2.1 Prior Knowledge

According to [1], as for a nonlinear system with  $x$ ,  $u$ , and  $y$  as the state, control input, and output vectors, the definition of passivity is as follows:

**Definition 1** The nonlinear system is passive, if there is a energy function  $\mathcal{H}$ , such that

$$\mathcal{H}(x(T)) \leq \mathcal{H}(x(0)) + \int_0^T h(u(t), y(t))dt \tag{1}$$

with  $h(u, y) = u^T y$  and any  $T \geq 0$ ; it is input strictly passive (ISP) if  $h(u, y) = u^T y - \delta_i \|u\|^2$  in (1), where  $\delta_i > 0$ ; the nonlinear system is output strictly passive (OSP) if  $h(u, y) = u^T y - \delta_o \|y\|^2$  in (1), where  $\delta_o > 0$ .

Moreover, passivity establishes the natural relationship with  $\mathcal{L}_2$  stability as follows [1]:

**Definition 2** The nonlinear system is said to be  $\mathcal{L}_2$  stable, if there exists a positive constant  $\epsilon$  such that for any initial condition  $x_0$  and  $T \geq 0$ , following inequality is satisfied with a finite constant  $\alpha(x_0)$ :

$$\left[ \int_0^T \|y(t)\|^2 dt \right]^{\frac{1}{2}} \leq \epsilon \left[ \int_0^T \|u(t)\|^2 dt \right]^{\frac{1}{2}} + \alpha(x_0).$$

**Lemma 1** If the nonlinear system is OSP, then it is  $\mathcal{L}_2$  stable.

### 2.2 General IDA-PBC

Classical PBC always focuses on the dynamics modelled by Euler-Lagrange (EL) equation as follows with ignored  $t$  for simplified representation, which describes the behaviour of a large class of engineering systems:

$$\mathcal{M}(q)\ddot{q} + \mathcal{C}(q, \dot{q})\dot{q} + \frac{\partial \mathcal{V}(q)}{\partial q} = \mathcal{B}(q)u + d,$$

where  $q(t) \in \mathbb{R}^n$  is the generalized position vector,  $\mathcal{M}(q)$  is the generalized inertial matrix,  $\mathcal{C}(q, \dot{q}) = \dot{\mathcal{M}}(q) - \frac{1}{2} \frac{\partial \dot{q}^T \mathcal{M}(q)}{\partial q}$ ,  $\mathcal{V}(q)$  is the potential energy function,  $\mathcal{B}(q)$  represents the input matrix that is usually an invertible matrix indicating fully-actuated system or a column full rank matrix indicating underactuated system,  $u(t) \in \mathbb{R}^m$  is the control input vector, and  $d(t)$  is the disturbance vector with Euclidean norm  $\|d(t)\| \leq T_d$ . To shape the total energy of the controlled plant by IDA-PBC, following port-controlled Hamiltonian (PCH) model is required [3], and EL equation could also be transformed into this form:

$$\begin{bmatrix} \dot{q} \\ \dot{p} \end{bmatrix} = \begin{bmatrix} 0 & I_n \\ -I_n & 0 \end{bmatrix} \begin{bmatrix} \nabla_q \mathcal{H} \\ \nabla_p \mathcal{H} \end{bmatrix} + \begin{bmatrix} 0 \\ \mathcal{B}(q) \end{bmatrix} u + \begin{bmatrix} 0 \\ d \end{bmatrix}, \tag{2}$$

where  $p(t) = \mathcal{M}(q(t))\dot{q}(t)$  is the generalized momenta, the Hamiltonian function  $\mathcal{H}(q, p) = \frac{1}{2} p^T \mathcal{M}^{-1}(q) p + \mathcal{V}(q)$  represents the total energy with gradients  $\nabla_q \mathcal{H} = -\frac{1}{2} \nabla_q \dot{q}^T \mathcal{M}(q) \dot{q} + \nabla_q \mathcal{V}(q)$  and  $\nabla_p \mathcal{H} = \mathcal{M}^{-1}(q) p$ , and the output vector is usually defined as  $y(t) = [q^T(t) \ p^T(t)]^T$  for state feedback control.

According to [2] and [3], the control input from IDA-PBC is proposed as

$$u = u_{di}(q, p) + u_{es}(q, p), \tag{3}$$

where  $u_{di}(q, p) = -K_d \mathcal{B}^T(q) \nabla_p \mathcal{H}_d$  injects damping, and  $\mathcal{B}(q)u_{es}(q, p) = \nabla_q \mathcal{H} - \mathcal{M}_d(q)\mathcal{M}^{-1}(q)\nabla_q \mathcal{H}_d + J_d \mathcal{M}_d^{-1}(q)p$  shapes energy with  $K_d > 0$  and  $J_d = -J_d^T$ . The desired Hamiltonian function is as follows with

$$q_* = \arg \min \mathcal{H}_d(q, p) = \arg \min \mathcal{V}_d(q) \text{ i.e. } \nabla_q \mathcal{V}_d(q_*) = 0, \nabla_q^2 \mathcal{V}_d(q_*) > 0. \tag{5}$$

Moreover, to deal with the underactuated system without an invertible input matrix, following partial differential equation (PDE) should be satisfied:

$$\mathcal{B}^\perp(q) \left[ \nabla_q \mathcal{H} - \mathcal{M}_d(q)\mathcal{M}^{-1}(q)\nabla_q \mathcal{H}_d + J_d \mathcal{M}_d^{-1}(q)p \right] = 0, \tag{6}$$

where  $\mathcal{B}^\perp(q)$  satisfies  $\mathcal{B}^\perp(q)\mathcal{B}(q) = 0$ .

By introducing (3) into (2), the desired PCH model and also the closed-loop system is as follows:

$$\begin{bmatrix} \dot{q} \\ \dot{p} \end{bmatrix} = (M_{es} - M_{di}) \begin{bmatrix} \nabla_q \mathcal{H}_d \\ \nabla_p \mathcal{H}_d \end{bmatrix} + \begin{bmatrix} 0 \\ d \end{bmatrix}, \tag{7}$$

where  $M_{es} = -M_{es}^T = \begin{bmatrix} 0 & \mathcal{M}^{-1}\mathcal{M}_d \\ -\mathcal{M}_d\mathcal{M}^{-1} & J_d \end{bmatrix}$  is from the item  $u_{es}$  in (3) for energy shaping, and  $M_{di} = M_{di}^T = \begin{bmatrix} 0 & 0 \\ 0 & \mathcal{B}(q)K_d\mathcal{B}^T(q) \end{bmatrix} \geq 0$  injects damping for  $\nabla_p \mathcal{H}_d$  by the item  $u_{di}$  in (3). The stability analysis could refer to [3].

### 3 Main Results

#### 3.1 Problem Statement

This section will consider the IDA-PBC under loss of actuator effectiveness for following simplified PCH model defined from (2):

$$\begin{bmatrix} \dot{q} \\ \dot{p} \end{bmatrix} = \begin{bmatrix} 0 & I_n \\ -I_n & 0 \end{bmatrix} \begin{bmatrix} \nabla_q \mathcal{H} \\ \nabla_p \mathcal{H} \end{bmatrix} + \begin{bmatrix} 0 \\ \mathcal{B} \end{bmatrix} \Gamma u + \begin{bmatrix} 0 \\ d \end{bmatrix},$$

$$y \triangleq \begin{bmatrix} q \\ p \end{bmatrix} = \begin{bmatrix} I_n & 0 \\ 0 & \mathcal{M}(q) \end{bmatrix} \begin{bmatrix} q \\ \dot{q} \end{bmatrix}, \tag{8}$$

where the Hamiltonian function  $\mathcal{H}(q, p) = \frac{1}{2}p^T \mathcal{M}^{-1}(q)p$  is with the simplified form, and  $\Gamma(t) = \text{diag}(\gamma_1(t), \dots, \gamma_m(t))$  with  $0 < \gamma I_m \leq \Gamma(t) \leq I_m$  represents loss of actuator effectiveness that could be time-varying. To avoid complex PDE (6) in controller design, the input matrix is assumed to be constant and with right inverse matrix  $\mathcal{B}^-$  that satisfies  $\mathcal{B} \cdot \mathcal{B}^- = I_n$  and  $\mathcal{B}^{-T} \cdot \mathcal{B}^T = I_n$ . In addition, the potential energy function  $\mathcal{V}(q)$  in the

$\mathcal{M}_d(q) > 0$  and  $\mathcal{V}_d(q) \geq 0$  as the desired inertia matrix and potential energy:

$$\mathcal{H}_d(q, p) = \frac{1}{2}p^T \mathcal{M}_d^{-1}(q)p + \mathcal{V}_d(q). \tag{4}$$

To achieve the tracking control towards a reference vector  $q_*$ , the desired potential energy function should have an isolated minimum:

simplified Hamiltonian function is further assumed to be zero to avoid the energy compensation under faults. Due to the common potential energy in mechanisms is induced by gravity, elasticity, and gravitation, the case with zero potential energy is usual in the attitude dynamics of most unmanned vehicles [5, 6]. Based on the lower bound of actuator faults represented by  $\gamma$ , following high-gain IDA-PBC would deal with the FTC problem of (8).

However, in the case without the known value of  $\gamma$ , high-gain IDA-PBC cannot work, and some new FTC methods should be designed. Moreover, the loss of actuator effectiveness always reduces the actuator saturation magnitudes. To further consider actuator saturation, the control input vector in (8) could be redefined as follows:

$$u = \text{sat}(v) = \begin{cases} [v_1 \dots v_m]^T, & |v_i| \leq u_{\max i} \\ [\text{sign}(v_1)u_{\max 1} \dots \text{sign}(v_m)u_{\max m}]^T, & |v_i| > u_{\max i} \end{cases} \tag{9}$$

with  $v$  as the outputs of controller and inputs of actuators,  $i = 1, \dots, m$ , and  $u_{\max} = [u_{\max 1} \dots u_{\max m}]^T$  as the saturation magnitude. According to (8) and (9), the form of  $\Gamma u = \Gamma \text{sat}(v)$  means the actuator faults could affect the actuator saturation magnitudes [13]. Due to the inputs for actuators are always finite in real platforms, the maximum outputs of actuators are limited by the actuator faults absolutely, so the form of  $\Gamma \text{sat}(v)$  is with practical significance actually. Under unknown actuator faults, following adaptive IDA-PBC would deal with the FTC problem of (8), and an auxiliary state vector would be introduced to allow the existence of the actuator saturation (9).

#### 3.2 High-gain IDA-PBC

According to (7), general IDA-PBC only injects damping for  $\nabla_p \mathcal{H}_d$ . To introduce damping into all states for the stability analysis in this section, consider the state transformation [21]:

$$z_q = q, z_p = p + \mathcal{B}K_q \mathcal{B}^T \mathcal{M}^{-1}(q) \nabla_{z_q} \mathcal{H}_d \tag{10}$$

with  $K_q > 0$  and following desired Hamiltonian function:

$$\mathcal{H}_d(z_q, z_p) = \frac{1}{2}z_p^T \mathcal{M}_d^{-1}z_p + \frac{1}{2}(z_q - q_*)^T K_p (z_q - q_*), \tag{11}$$

where  $q_*$  is a reference vector,  $\mathcal{M}_d$  is the constant desired inertial matrix, and  $K_p > 0$ . A closed-loop PCH system could be formulated as follows:

$$\begin{bmatrix} \dot{z}_q \\ \dot{z}_p \end{bmatrix} = \begin{bmatrix} -\mathcal{M}^{-1}(q)\mathcal{B}K_q\mathcal{B}^T\mathcal{M}^{-1}(q) & \mathcal{M}^{-1}(q)\mathcal{M}_d \\ -\mathcal{M}_d\mathcal{M}^{-1}(q) & -\mathcal{B}K_d\mathcal{B}^T \end{bmatrix} \begin{bmatrix} \nabla_{z_q}\mathcal{H}_d \\ \nabla_{z_p}\mathcal{H}_d \end{bmatrix} + \begin{bmatrix} 0 \\ \mathcal{B} \end{bmatrix} [\Gamma(t) - I_m]u + \begin{bmatrix} 0 \\ d(t) \end{bmatrix} \quad (12)$$

where following control input vector is introduced into (8) with  $\mathcal{B}\Gamma(t)u = \mathcal{B}u + \mathcal{B}[\Gamma(t) - I_m]u$ :

$$\begin{aligned} u &= \mathcal{B}^{-1}\nabla_q\mathcal{H} - \mathcal{B}^{-1}\mathcal{M}_d\mathcal{M}^{-1}(q)\nabla_{z_q}\mathcal{H}_d \\ &\quad - K_d\mathcal{B}^T\nabla_{z_p}\mathcal{H}_d - K_q\mathcal{B}^T\frac{d[\mathcal{M}^{-1}(q)\nabla_{z_q}\mathcal{H}_d]}{dt} \\ &= -K_d\mathcal{B}^T\nabla_{z_p}\mathcal{H}_d - \left[ \mathcal{B}^{-1}\mathcal{M}_d - K_q\mathcal{B}^T\mathcal{M}^{-1}(q)\dot{\mathcal{M}}(q) \right] \mathcal{M}^{-1}(q)\nabla_{z_q}\mathcal{H}_d \\ &\quad - \left[ \frac{1}{2}\mathcal{B}^{-1}\frac{\partial\dot{q}^T\mathcal{M}(q)}{\partial q} + K_q\mathcal{B}^T\mathcal{M}^{-1}(q)K_p \right] \dot{q}, \end{aligned} \quad (13)$$

with  $\dot{q} = \mathcal{M}^{-1}(q)\mathcal{M}_d\nabla_{z_p}\mathcal{H}_d - \mathcal{M}^{-1}(q)\mathcal{B}K_q\mathcal{B}^T\mathcal{M}^{-1}(q)\nabla_{z_q}\mathcal{H}_d$ . Compared with (4) for general IDA-PBC, (11) is with constant  $\mathcal{M}_d$  and  $\mathcal{V}_d(q) = \frac{1}{2}(z_q - q_*)^T K_p(z_q - q_*)$ , and  $J_d$  in (3) is set as 0 in (13) for simplification. Obviously, the control law (13) is absolutely available in fault-free case ( $\Gamma(t) = I_m$ ) [21]. With following theorem, this control law

could ensure the  $\mathcal{L}_2$  stability of (8) under loss of actuator effectiveness.

**Theorem 1** *With the control input vector (13), if the lower bound of actuator faults  $\gamma$  is known, and there exist parameters  $\sigma_1 > 0$ ,  $\sigma_2 > 0$ , and  $\sigma_3 > 0$ , matrices  $\mathcal{M}_d$ ,  $K_q$ , and  $K_p$ , and a diagonal matrix  $K_d$  that satisfy following inequalities for two intermediate matrices  $M_1$  and  $M_2$ :*

$$\begin{aligned} \frac{1}{2\sigma_1}Mu &\left\{ \left[ \frac{1}{2}\mathcal{B}^{-1}\frac{\partial\dot{q}^T\mathcal{M}(q)}{\partial q} + K_q\mathcal{B}^T\mathcal{M}^{-1}(q)K_p \right] \mathcal{M}^{-1}(q)\mathcal{M}_d\mathcal{B}^{-T} \right\} \leq M_1, \\ \frac{1}{2\sigma_2}Mu &\left[ \mathcal{B}^{-1}\mathcal{M}_d - K_q\mathcal{B}^T\mathcal{M}^{-1}(q)\dot{\mathcal{M}}(q) \right] + \\ \frac{1}{2\sigma_3}Mu &\left\{ \left[ \frac{1}{2}\mathcal{B}^{-1}\frac{\partial\dot{q}^T\mathcal{M}(q)}{\partial q} + K_q\mathcal{B}^T\mathcal{M}^{-1}(q)K_p \right] \mathcal{M}^{-1}(q)\mathcal{B}K_q\mathcal{B}^T \right\} \leq M_2, \end{aligned} \quad (14)$$

$$\mathcal{M}_d > 0, \quad \gamma K_d > \frac{\sigma_1 + \sigma_2 + \sigma_3}{2}(1 - \gamma)^2 I_m + M_1, \quad \mathcal{B}K_q\mathcal{B}^T \geq M_2, \quad K_p > 0, \quad (15)$$

then, for closed-loop system (12), the map  $d(t) \mapsto \nabla_{z_p}\mathcal{H}_d$  is  $\mathcal{L}_2$  stable under the loss of actuator effectiveness  $\Gamma(t)$  that satisfies  $0 < \gamma I_m \leq \Gamma(t) \leq I_m$ .

*Proof* Regard (11) as the Lyapunov function, and consider its derivative with (12):

$$\begin{aligned} \dot{\mathcal{H}}_d &= \begin{bmatrix} \nabla_{z_q}^T\mathcal{H}_d & \nabla_{z_p}^T\mathcal{H}_d \end{bmatrix} \begin{bmatrix} \dot{z}_q \\ \dot{z}_p \end{bmatrix} \\ &= -\nabla_{z_q}^T\mathcal{H}_d\mathcal{M}^{-1}(q)\mathcal{B}K_q\mathcal{B}^T\mathcal{M}^{-1}(q)\nabla_{z_q}\mathcal{H}_d - \nabla_{z_p}^T\mathcal{H}_d\mathcal{B}K_d\mathcal{B}^T\nabla_{z_p}\mathcal{H}_d \\ &\quad + \nabla_{z_p}^T\mathcal{H}_d\mathcal{B}[\Gamma(t) - I_m]u + \nabla_{z_p}^T\mathcal{H}_dd(t). \end{aligned}$$

Then introduce (13) into above equation, and there is:

$$\begin{aligned} \dot{\mathcal{H}}_d &= \begin{bmatrix} \nabla_{z_q}^T \mathcal{H}_d & \nabla_{z_p}^T \mathcal{H}_d \end{bmatrix} \begin{bmatrix} \dot{z}_q \\ \dot{z}_p \end{bmatrix} \\ &= -\nabla_{z_q}^T \mathcal{H}_d \mathcal{M}^{-1}(q) \mathcal{B} K_q \mathcal{B}^T \mathcal{M}^{-1}(q) \nabla_{z_q} \mathcal{H}_d - \nabla_{z_p}^T \mathcal{H}_d \mathcal{B} \Gamma(t) K_d \mathcal{B}^T \nabla_{z_p} \mathcal{H}_d \\ &\quad + \nabla_{z_p}^T \mathcal{H}_d d(t) + \tilde{H}, \end{aligned} \tag{16}$$

where

$$\begin{aligned} \tilde{H} &= \nabla_{z_p}^T \mathcal{H}_d \mathcal{B} [I_m - \Gamma(t)] \left[ \mathcal{B}^- \mathcal{M}_d - K_q \mathcal{B}^T \mathcal{M}^{-1}(q) \dot{\mathcal{M}}(q) \right] \mathcal{M}^{-1}(q) \nabla_{z_q} \mathcal{H}_d - \\ &\quad \nabla_{z_p}^T \mathcal{H}_d \mathcal{B} [I_m - \Gamma(t)] \left[ \frac{1}{2} \mathcal{B}^- \frac{\partial \dot{q}^T \mathcal{M}(q)}{\partial q} + K_q \mathcal{B}^T \mathcal{M}^{-1}(q) K_p \right] \mathcal{M}^{-1}(q) \mathcal{B} K_q \cdot \\ &\quad \mathcal{B}^T \mathcal{M}^{-1}(q) \nabla_{z_q} \mathcal{H}_d + \nabla_{z_p}^T \mathcal{H}_d \mathcal{B} [I_m - \Gamma(t)] \cdot \\ &\quad \left[ \frac{1}{2} \mathcal{B}^- \frac{\partial \dot{q}^T \mathcal{M}(q)}{\partial q} + K_q \mathcal{B}^T \mathcal{M}^{-1}(q) K_p \right] \mathcal{M}^{-1}(q) \mathcal{M}_d \nabla_{z_p} \mathcal{H}_d. \end{aligned}$$

Note that, for any vector  $x$  and  $y$ , following inequality is satisfied for any parameter  $\sigma > 0$ :

$$x^T y \leq \frac{1}{2\sigma} x^T x + \frac{\sigma}{2} y^T y. \tag{17}$$

Based on this inequality,  $\tilde{H}$  could be relaxed with  $\sigma_1 > 0$ ,  $\sigma_2 > 0$ , and  $\sigma_3 > 0$ . Due to  $0 < \gamma I_m \leq \Gamma(t) \leq I_m$  with known  $\gamma$ ,  $[I_m - \Gamma(t)]^T [I_m - \Gamma(t)] \leq (1 - \gamma)^2 I_m$  is satisfied, and  $\tilde{H}$  is with following form according to (14) and (17):

$$\begin{aligned} \tilde{H} &\leq \frac{1}{2\sigma_1} \nabla_{z_p}^T \mathcal{H}_d \mathcal{B} \cdot \text{Mu} \left\{ \left[ \frac{1}{2} \mathcal{B}^- \frac{\partial \dot{q}^T \mathcal{M}(q)}{\partial q} + K_q \mathcal{B}^T \mathcal{M}^{-1}(q) K_p \right] \mathcal{M}^{-1}(q) \mathcal{M}_d \right. \\ &\quad \left. \mathcal{B}^T \right\} \cdot \mathcal{B}^T \nabla_{z_p} \mathcal{H}_d + \frac{\sigma_1}{2} \nabla_{z_p}^T \mathcal{H}_d \mathcal{B} [I_m - \Gamma(t)] [I_m - \Gamma(t)] \mathcal{B}^T \nabla_{z_p} \mathcal{H}_d + \\ &\quad \frac{1}{2\sigma_2} \nabla_{z_q}^T \mathcal{H}_d \mathcal{M}^{-1}(q) \cdot \text{Mu} \left[ \mathcal{B}^- \mathcal{M}_d - K_q \mathcal{B}^T \mathcal{M}^{-1}(q) \dot{\mathcal{M}}(q) \right] \cdot \\ &\quad \mathcal{M}^{-1}(q) \nabla_{z_q} \mathcal{H}_d + \frac{\sigma_2}{2} \nabla_{z_p}^T \mathcal{H}_d \mathcal{B} [I_m - \Gamma(t)] [I_m - \Gamma(t)] \mathcal{B}^T \nabla_{z_p} \mathcal{H}_d + \\ &\quad \frac{1}{2\sigma_3} \nabla_{z_q}^T \mathcal{H}_d \mathcal{M}^{-1}(q) \cdot \text{Mu} \left\{ \left[ \frac{1}{2} \mathcal{B}^- \frac{\partial \dot{q}^T \mathcal{M}(q)}{\partial q} + K_q \mathcal{B}^T \mathcal{M}^{-1}(q) K_p \right] \mathcal{M}^{-1}(q) \right. \\ &\quad \left. \mathcal{B} K_q \mathcal{B}^T \right\} \cdot \mathcal{M}^{-1}(q) \nabla_{z_q} \mathcal{H}_d + \\ &\quad \frac{\sigma_3}{2} \nabla_{z_p}^T \mathcal{H}_d \mathcal{B} [I_m - \Gamma(t)] [I_m - \Gamma(t)] \mathcal{B}^T \nabla_{z_p} \mathcal{H}_d \\ &\leq \nabla_{z_q}^T \mathcal{H}_d \mathcal{M}^{-1}(q) \cdot M_2 \cdot \mathcal{M}^{-1}(q) \nabla_{z_q} \mathcal{H}_d + \\ &\quad \nabla_{z_p}^T \mathcal{H}_d \mathcal{B} \left[ \frac{\sigma_1 + \sigma_2 + \sigma_3}{2} (1 - \gamma)^2 I_m + M_1 \right] \mathcal{B}^T \nabla_{z_p} \mathcal{H}_d. \end{aligned}$$

By introducing above equation into (16), the derivative of  $\mathcal{H}_d(z_q, z_p)$  could be reformulated with diagonal matrix  $K_d$ :

$$\begin{aligned} \dot{\mathcal{H}}_d &\leq -\nabla_{z_q}^T \mathcal{H}_d \mathcal{M}^{-1}(q) \left( \mathcal{B} K_q \mathcal{B}^T - M_2 \right) \mathcal{M}^{-1}(q) \nabla_{z_q} \mathcal{H}_d + \nabla_{z_p}^T \mathcal{H}_d d(t) \\ &\quad - \nabla_{z_p}^T \mathcal{H}_d \mathcal{B} \left[ \gamma K_d - \frac{\sigma_1 + \sigma_2 + \sigma_3}{2} (1 - \gamma)^2 I_m - M_1 \right] \mathcal{B}^T \nabla_{z_p} \mathcal{H}_d. \end{aligned}$$

Based on (15), above equation could be formulated as follows:

$$\begin{aligned} \dot{\mathcal{H}}_d \leq & -\nabla_{z_p}^T \mathcal{H}_d \mathcal{B} \left[ \gamma K_d - \frac{\sigma_1 + \sigma_2 + \sigma_3}{2} (1 - \gamma)^2 I_m - M_1 \right] \mathcal{B}^T \nabla_{z_p} \mathcal{H}_d \\ & + \nabla_{z_p}^T \mathcal{H}_d d(t). \end{aligned} \tag{18}$$

Due to  $\mathcal{B} \left[ \gamma K_d - \frac{\sigma_1 + \sigma_2 + \sigma_3}{2} (1 - \gamma)^2 I_m - M_1 \right] \mathcal{B}^T > 0$ , according to Definition 1, (18) means the closed-loop system (12) is OSP. Based on Lemma 1, the  $\mathcal{L}_2$  stability defined in Definition 2 is satisfied, so the map  $d(t) \mapsto \nabla_{z_p} \mathcal{H}_d$  is  $\mathcal{L}_2$  stable under the loss of actuator effectiveness  $\Gamma(t)$ .  $\square$

*Remark 1* Above theorem increases the gains of  $K_d$  and  $K_q$  based on the lower bound of actuator faults and intermediate matrices  $M_1$  and  $M_2$ . In the applications of Theorem 1, the values of  $M_1$ ,  $M_2$ ,  $\mathcal{M}_d$ , and  $K_p$  could be given directly. To determine the values of  $\sigma_1$ ,  $\sigma_2$ ,  $\sigma_3$ ,  $K_q$ , and  $K_d$  that satisfy (14) and (15), the following forms could be considered online:

$$\begin{aligned} \sigma_1 &= \frac{1}{2\lambda_{\min}(M_1)} (\lambda_{\max} \cdot \text{Mu}) \left\{ \left[ \frac{1}{2} \mathcal{B}^- \frac{\partial \dot{q}^T \mathcal{M}(q)}{\partial q} + K_q \mathcal{B}^T \mathcal{M}^{-1}(q) K_p \right] \right. \\ &\quad \left. \mathcal{M}^{-1}(q) \mathcal{M}_d \mathcal{B}^{-T} \right\}, \\ \sigma_2 &= \frac{1}{\lambda_{\min}(M_2)} (\lambda_{\max} \cdot \text{Mu}) \left[ \mathcal{B}^- \mathcal{M}_d - K_q \mathcal{B}^T \mathcal{M}^{-1}(q) \dot{\mathcal{M}}(q) \right], \\ \sigma_3 &= \frac{1}{\lambda_{\min}(M_2)} (\lambda_{\max} \cdot \text{Mu}) \left\{ \left[ \frac{1}{2} \mathcal{B}^- \frac{\partial \dot{q}^T \mathcal{M}(q)}{\partial q} + K_q \mathcal{B}^T \mathcal{M}^{-1}(q) K_p \right] \right. \\ &\quad \left. \mathcal{M}^{-1}(q) \mathcal{B} K_q \mathcal{B}^T \right\}. \end{aligned} \tag{19}$$

The above  $\sigma_1$ ,  $\sigma_2$ , and  $\sigma_3$  ensure the satisfaction of (14), where  $K_q$  could be obtained by  $\mathcal{B} K_q \mathcal{B}^T \geq M_2$  directly, and  $K_d$  must be determined online by  $\gamma K_d > \frac{\sigma_1 + \sigma_2 + \sigma_3}{2} (1 - \gamma)^2 I_m + M_1$  according to (15). It could be noticed that  $K_d$  would be time-varying based on the parameters from (19). According to the proof, the time-varying  $K_d$  has no effect on the stability analysis. However, other parameter matrices, such as  $\mathcal{M}_d$ ,  $K_q$ , and  $K_p$ , must be constant in case of introducing corresponding derivatives, which are difficult to handle with.

controller gains always aim at the worst faulty case, and own simpler controller structures compared with active FTC methods. However, they are absolutely conservative without considering the real-time fault magnitudes, and this is a general disadvantage of passive FTC methods. Moreover, compared with fault-free case, the high-gain controllers for faulty case, such as high-gain IDA-PBC, are more possible to induce actuator saturation. Following subsection would consider this issue without the prior information about loss of actuator effectiveness and its lower bound.

In this subsection, high-gain IDA-PBC is proposed to deal with the loss of actuator effectiveness, and the lower bound of actuator faults is applied in order to improve the nominal controller performance, which is similar to some existing passive FTC methods based on high-gain idea [9, 10, 18, 23]. These FTC methods based on high

### 3.3 Adaptive IDA-PBC

To deal with actuator saturation under loss of actuator effectiveness, introduce control input vector  $v = v_1 + v_2$  into (8) with  $\mathcal{B}\Gamma(t)u = \mathcal{B}v + \mathcal{B}(u - v) + \mathcal{B}[\Gamma(t) - I_m]u$ , where

$$\begin{aligned} v_1 &= \mathcal{B}^- \left[ \nabla_q \mathcal{H} - \mathcal{M}_d(q) \mathcal{M}^{-1}(q) \nabla_{z_q} \mathcal{H}_d \right] + \mathcal{B}^- J_d \nabla_{z_p} \mathcal{H}_d - K_d \mathcal{B}^T \nabla_{z_p} \mathcal{H}_d \\ &\quad - K_q \mathcal{B}^T \frac{d[\mathcal{M}^{-1}(q) \nabla_{z_q} \mathcal{H}_d]}{dt} \end{aligned} \tag{20}$$



with  $z_q$  and  $z_p$  defined in (10), and  $v_2$  is an adaptive control input vector that would be designed in this subsection. Then following PCH system could be formulated with  $\Delta u = u - v$ :

$$\begin{bmatrix} \dot{z}_q \\ \dot{z}_p \end{bmatrix} = \begin{bmatrix} -\mathcal{M}^{-1}(q)\mathcal{B}K_q\mathcal{B}^T\mathcal{M}^{-1}(q) & \mathcal{M}^{-1}(q)\mathcal{M}_d(q) \\ -\mathcal{M}_d(q)\mathcal{M}^{-1}(q) & J_d - \mathcal{B}K_d\mathcal{B}^T \end{bmatrix} \begin{bmatrix} \nabla_{z_q}\mathcal{H}_d \\ \nabla_{z_p}\mathcal{H}_d \end{bmatrix} + \begin{bmatrix} 0 \\ \mathcal{B} \end{bmatrix} v_2 + \begin{bmatrix} 0 \\ \mathcal{B} \end{bmatrix} \Delta u + \begin{bmatrix} 0 \\ \mathcal{B} \end{bmatrix} [\Gamma(t) - I_m]u + \begin{bmatrix} 0 \\ d(t) \end{bmatrix}, \quad (21)$$

where the desired Hamiltonian function is equal to

$$\mathcal{H}_d(z_q, z_p) = \frac{1}{2}z_p^T\mathcal{M}_d^{-1}(z_q)z_p + \mathcal{V}_d(z_q) \quad (22)$$

with  $\mathcal{M}_d(z_q) > 0$  and  $\mathcal{V}_d(z_q) > 0$  satisfying (5). Note that (13) and (11) are actually the special forms of (20) and (22) with  $\mathcal{M}_d(z_q) = \mathcal{M}_d$ ,  $\mathcal{V}_d(z_q) = \frac{1}{2}(z_q - q_*)^T K_p(z_q - q_*)$ , and  $J_d = 0$ .

To deal with  $\Delta u$ ,  $[\Gamma(t) - I_m]u$ , and  $d(t)$  in (21) by  $v_2$ , following adaptive control input vector is formed:

$$v_2 = K_a x_a - \mathcal{B}^{-1} \frac{\nabla_{z_p}\mathcal{H}_d}{\|\nabla_{z_p}\mathcal{H}_d\|} \left[ \hat{T}_d + \sqrt{\lambda_{\max}(\mathcal{B}^T\mathcal{B})u_{\max}^T u_{\max}(1 - \hat{\gamma})} \right], \quad (23)$$

where an auxiliary state vector  $x_a \in \mathbb{R}^m$  and two parameters are required dependent on  $T_d \geq 0$  and  $\gamma \leq 1$  as follows:

$$\dot{x}_a = -k_a x_a - \frac{\nabla_{z_p}^T \mathcal{H}_d \mathcal{B} \Delta u}{x_a^T x_a} x_a, \quad (k_a > 0), \quad (24)$$

$$\dot{\hat{T}}_d = k_d \|\nabla_{z_p}\mathcal{H}_d\|, \quad (\hat{T}_d(0) \geq 0, k_d > 0),$$

$$\dot{\hat{\gamma}} = -k_\gamma \|\nabla_{z_p}\mathcal{H}_d\| \sqrt{\lambda_{\max}(\mathcal{B}^T\mathcal{B})u_{\max}^T u_{\max}}, \quad (\hat{\gamma}(0) \leq 1, k_\gamma > 0). \quad (25)$$

The vector  $x_a$  is applied to deal with  $\Delta u$  in (21). Based on (24), the actuator saturation is allowed in controller applications [13], and the saturated control inputs could ensure the asymptotic stability according to following theorem.

**Theorem 2** *With the control input vectors (20) and (23) based on the parameters in (25), if there exist parameters  $\sigma_a > 0$ ,  $k_a > \frac{\sigma_a}{2}$ ,  $k_d > 0$ , and  $k_\gamma > 0$ , matrices  $K_q$ ,  $K_d$ , and  $K_a$  that satisfy  $K_d > \frac{1}{2\sigma_a} K_a K_a^T > 0$  and  $K_q > 0$ , then the asymptotic stability of  $\nabla_{z_q}\mathcal{H}_d$ ,  $\nabla_{z_p}\mathcal{H}_d$ , and  $x_a$  could be ensured for the controlled plant (8) with actuator saturation (9) and the unknown lower bound of actuator faults.*

*Proof* Define  $\tilde{T}_d = \hat{T}_d - T_d$ ,  $\tilde{\gamma} = \hat{\gamma} - \gamma$ , and  $\mathcal{V}_{\text{Lya}} = \mathcal{H}_d(z_q, z_p) + \frac{1}{2}x_a^T x_a + \frac{1}{2k_d}\tilde{T}_d^2 + \frac{1}{2k_\gamma}\tilde{\gamma}^2$  as Lyapunov function. Consider the derivative of this Lyapunov function with system (21):

$$\begin{aligned} \dot{\mathcal{V}}_{\text{Lya}} &= \dot{\mathcal{H}}_d(z_q, z_p) + x_a^T \dot{x}_a + \frac{1}{k_d}\tilde{T}_d\dot{\tilde{T}}_d + \frac{1}{k_\gamma}\tilde{\gamma}\dot{\tilde{\gamma}} \\ &= -\nabla_{z_q}^T \mathcal{H}_d \mathcal{M}^{-1}(q)\mathcal{B}K_q\mathcal{B}^T\mathcal{M}^{-1}(q)\nabla_{z_q}\mathcal{H}_d - \nabla_{z_p}^T \mathcal{H}_d \mathcal{B}K_d\mathcal{B}^T\nabla_{z_p}\mathcal{H}_d \\ &\quad + \nabla_{z_p}^T \mathcal{H}_d \mathcal{B}v_2 + \nabla_{z_p}^T \mathcal{H}_d \mathcal{B}\Delta u + \nabla_{z_p}^T \mathcal{H}_d \mathcal{B}[\Gamma(t) - I_m]u + \nabla_{z_p}^T \mathcal{H}_d d(t) \\ &\quad + x_a^T \left( -k_a x_a - \frac{\nabla_{z_p}^T \mathcal{H}_d \mathcal{B} \Delta u}{x_a^T x_a} x_a \right) + \frac{1}{k_d}\tilde{T}_d\dot{\tilde{T}}_d + \frac{1}{k_\gamma}\tilde{\gamma}\dot{\tilde{\gamma}} \\ &\leq -\nabla_{z_q}^T \mathcal{H}_d \mathcal{M}^{-1}(q)\mathcal{B}K_q\mathcal{B}^T\mathcal{M}^{-1}(q)\nabla_{z_q}\mathcal{H}_d - k_a x_a^T x_a \\ &\quad - \nabla_{z_p}^T \mathcal{H}_d \mathcal{B}K_d\mathcal{B}^T\nabla_{z_p}\mathcal{H}_d + \nabla_{z_p}^T \mathcal{H}_d \mathcal{B}v_2 + \|\nabla_{z_p}\mathcal{H}_d\| \cdot \|d(t)\| \\ &\quad + \|\nabla_{z_p}\mathcal{H}_d\| \cdot \|\mathcal{B}[\Gamma(t) - I_m]u\| + \frac{1}{k_d}\tilde{T}_d\dot{\tilde{T}}_d + \frac{1}{k_\gamma}\tilde{\gamma}\dot{\tilde{\gamma}}. \end{aligned}$$

Then the adaptive control input vector  $v_2$  in (23) and parameters in (25) should be applied. Due to  $\gamma \leq 1$ , introduce

$$\|\mathcal{B}[\Gamma(t) - I_m]u\| \leq \sqrt{\lambda_{\max}(\mathcal{B}^T\mathcal{B})u_{\max}^T u_{\max}(1 - \hat{\gamma} + \tilde{\gamma})},$$

$$\|d(t)\| \leq T_d = \hat{T}_d - \tilde{T}_d, \quad \dot{\hat{T}}_d = \dot{\tilde{T}}_d, \quad \dot{\tilde{\gamma}} = \dot{\tilde{\gamma}},$$

parameters in (25), and  $v_2$  in (23) into above  $\dot{\mathcal{V}}_{\text{Lya}}$ , and following equation could be formulated:

$$\begin{aligned} \dot{\mathcal{V}}_{\text{Lya}} &\leq -\nabla_{z_q}^T \mathcal{H}_d \mathcal{M}^{-1}(q)\mathcal{B}K_q\mathcal{B}^T\mathcal{M}^{-1}(q)\nabla_{z_q}\mathcal{H}_d - \nabla_{z_p}^T \mathcal{H}_d \mathcal{B}K_d\mathcal{B}^T\nabla_{z_p}\mathcal{H}_d \\ &\quad - k_a x_a^T x_a + \nabla_{z_p}^T \mathcal{H}_d \mathcal{B}v_2 + \|\nabla_{z_p}\mathcal{H}_d\| \left[ \hat{T}_d + \sqrt{\lambda_{\max}(\mathcal{B}^T\mathcal{B})u_{\max}^T u_{\max}(1 - \hat{\gamma})} \right] \\ &= -\nabla_{z_q}^T \mathcal{H}_d \mathcal{M}^{-1}(q)\mathcal{B}K_q\mathcal{B}^T\mathcal{M}^{-1}(q)\nabla_{z_q}\mathcal{H}_d - \nabla_{z_p}^T \mathcal{H}_d \mathcal{B}K_d\mathcal{B}^T\nabla_{z_p}\mathcal{H}_d \\ &\quad - k_a x_a^T x_a + \nabla_{z_p}^T \mathcal{H}_d \mathcal{B}K_a x_a. \end{aligned}$$

Further apply (17) for

$$\nabla_{z_p}^T \mathcal{H}_d \mathcal{B} K_a x_a \leq \frac{1}{2\sigma_a} \nabla_{z_p}^T \mathcal{H}_d \mathcal{B} K_a K_a^T \mathcal{B}^T \nabla_{z_p} \mathcal{H}_d + \frac{\sigma_a}{2} x_a^T x_a,$$

and following equation could be formulated:

$$\begin{aligned} \dot{\mathcal{V}}_{\text{Lya}} &\leq -\nabla_{z_q}^T \mathcal{H}_d \mathcal{M}^{-1}(q) \mathcal{B} K_q \mathcal{B}^T \mathcal{M}^{-1}(q) \nabla_{z_q} \mathcal{H}_d \\ &\quad -\nabla_{z_p}^T \mathcal{H}_d \mathcal{B} \left( K_d - \frac{1}{2\sigma_a} K_a K_a^T \right) \mathcal{B}^T \nabla_{z_p} \mathcal{H}_d - \left( k_a - \frac{\sigma_a}{2} \right) x_a^T x_a \leq 0. \end{aligned}$$

According to invariant principle in [24], the closed-loop system would converge to the largest invariant set contained in the set with  $\dot{\mathcal{V}}_{\text{Lya}} = 0$ , which means  $\nabla_{z_q} \mathcal{H}_d = \nabla_{z_p} \mathcal{H}_d = x_a = 0$ . Consequently, the asymptotic stability of  $\nabla_{z_q} \mathcal{H}_d$ ,  $\nabla_{z_p} \mathcal{H}_d$ , and  $x_a$  could be achieved.  $\square$

*Remark 2* The asymptotic stability of  $\nabla_{z_p} \mathcal{H}_d$  means  $\lim_{t \rightarrow +\infty} \mathcal{M}_d^{-1}(z_q) z_p = \lim_{t \rightarrow +\infty} z_p = 0$ . Together with the stability of  $\nabla_{z_q} \mathcal{H}_d$ , the tracking of  $q$  towards  $q_*$  could be ensured. It is much easier to understand in the case

with  $\mathcal{V}_d(q) = \frac{1}{2}(q - q_*)^T K_p (q - q_*)$  and  $K_p > 0$ , and  $\lim_{t \rightarrow +\infty} \nabla_{z_q} \mathcal{H}_d = 0$  is equal to  $\lim_{t \rightarrow +\infty} K_d (q - q_*) = 0$ .

Due to the asymptotic stability of  $\nabla_{z_q} \mathcal{H}_d$ , the denominator in control law (23) approaches 0 with  $t \rightarrow +\infty$ . This phenomenon induces severe fluctuations of control inputs as shown in [9] and [14]. Note that the denominator in (24) has little effect on control inputs due to the integral relationship between  $\dot{x}_a$  and  $x_a$ . To deal with the denominator in (23), replace (23) and (25) by following adaptive control input vector and parameters:

$$v_2 = K_a x_a - \mathcal{B}^{-1} \frac{\nabla_{z_p} \mathcal{H}_d}{\|\nabla_{z_p} \mathcal{H}_d\| + \Sigma_{\mathcal{H}}} \left[ \hat{T}_d + \sqrt{\lambda_{\max}(\mathcal{B}^T \mathcal{B}) u_{\max}^T u_{\max}} (1 - \hat{\gamma}) \right], \tag{26}$$

$$\begin{aligned} \dot{\hat{T}}_d &= k_d \frac{\|\nabla_{z_p} \mathcal{H}_d\|}{\|\nabla_{z_p} \mathcal{H}_d\| + \Sigma_{\mathcal{H}}} \|\nabla_{z_p} \mathcal{H}_d\|, \quad (\hat{T}_d(0) \geq 0, k_d > 0), \\ \dot{\hat{\gamma}} &= -k_{\gamma} \frac{\|\nabla_{z_p} \mathcal{H}_d\|}{\|\nabla_{z_p} \mathcal{H}_d\| + \Sigma_{\mathcal{H}}} \|\nabla_{z_p} \mathcal{H}_d\| \sqrt{\lambda_{\max}(\mathcal{B}^T \mathcal{B}) u_{\max}^T u_{\max}}, \\ &\quad (\hat{\gamma}(0) \leq 1, k_{\gamma} > 0), \end{aligned} \tag{27}$$

where  $\Sigma_{\mathcal{H}}$  is a small positive constant. Following corollary would analyze the closed-loop property with modified control input vector (26) and parameters in (27).

**Corollary 1** *With the control input vectors (20) and (26) based on the parameters in (27), if there exist parameters  $\sigma_a > 0$ ,  $k_a > \frac{\sigma_a}{2}$ ,  $k_d > 0$ , and  $k_{\gamma} > 0$ , matrices  $K_q$ ,  $K_d$ ,*

*and  $K_a$  that satisfy  $K_d > \frac{1}{2\sigma_a} K_a K_a^T > 0$  and  $K_q > 0$ , then  $\nabla_{z_q} \mathcal{H}_d$ ,  $\nabla_{z_p} \mathcal{H}_d$ , and  $x_a$  would ultimately converge to the definite ranges from norm point of view for the controlled plant (8) with actuator saturation (9) and the unknown lower bound of actuator faults. Furthermore, if  $\mathcal{M}^{-1}(q)$  is with bounded eigenvalues, the definite ranges would also be bounded.*

*Proof* Similar to the proof of Theorem 2, define  $\tilde{T}_d = \hat{T}_d - T_d$ ,  $\tilde{\gamma} = \hat{\gamma} - \gamma$ , and  $\mathcal{V}_{\text{Lya}} = \mathcal{H}_d(z_q, z_p) + \frac{1}{2} x_a^T x_a + \frac{1}{2k_d} \tilde{T}_d^2 + \frac{1}{2k_{\gamma}} \tilde{\gamma}^2$  as Lyapunov function. Consider the derivative of this Lyapunov function with (24), (26), and (27):

$$\begin{aligned} \dot{\mathcal{V}}_{\text{Lya}} &= \dot{\mathcal{H}}_d(z_q, z_p) + x_a^T \dot{x}_a + \frac{1}{k_d} \tilde{T}_d \dot{\tilde{T}}_d + \frac{1}{k_{\gamma}} \tilde{\gamma} \dot{\tilde{\gamma}} \\ &\leq -\nabla_{z_q}^T \mathcal{H}_d \mathcal{M}^{-1}(q) \mathcal{B} K_q \mathcal{B}^T \mathcal{M}^{-1}(q) \nabla_{z_q} \mathcal{H}_d - \nabla_{z_p}^T \mathcal{H}_d \mathcal{B} K_d \mathcal{B}^T \nabla_{z_p} \mathcal{H}_d \\ &\quad -k_a x_a^T x_a + \nabla_{z_p}^T \mathcal{H}_d \mathcal{B} v_2 + \|\nabla_{z_p} \mathcal{H}_d\| (\hat{T}_d - \tilde{T}_d) \\ &\quad + \|\nabla_{z_p} \mathcal{H}_d\| \sqrt{\lambda_{\max}(\mathcal{B}^T \mathcal{B}) u_{\max}^T u_{\max}} (1 - \hat{\gamma} + \tilde{\gamma}) + \frac{1}{k_d} \tilde{T}_d \dot{\tilde{T}}_d + \frac{1}{k_{\gamma}} \tilde{\gamma} \dot{\tilde{\gamma}} \\ &= -\nabla_{z_q}^T \mathcal{H}_d \mathcal{M}^{-1}(q) \mathcal{B} K_q \mathcal{B}^T \mathcal{M}^{-1}(q) \nabla_{z_q} \mathcal{H}_d - \nabla_{z_p}^T \mathcal{H}_d \mathcal{B} K_d \mathcal{B}^T \nabla_{z_p} \mathcal{H}_d \\ &\quad -k_a x_a^T x_a + \nabla_{z_p}^T \mathcal{H}_d \mathcal{B} K_a x_a + \left( 1 - \frac{\|\nabla_{z_p} \mathcal{H}_d\|}{\|\nabla_{z_p} \mathcal{H}_d\| + \Sigma_{\mathcal{H}}} \right) \|\nabla_{z_p} \mathcal{H}_d\| [T_d \\ &\quad + \sqrt{\lambda_{\max}(\mathcal{B}^T \mathcal{B}) u_{\max}^T u_{\max}} (1 - \gamma)]. \end{aligned}$$



Then apply inequality (17), and following equation could be formulated:

$$\begin{aligned} \dot{V}_{Ly_a} &\leq -\nabla_{z_q}^T \mathcal{H}_d \mathcal{M}^{-1}(q) \mathcal{B} K_q \mathcal{B}^T \mathcal{M}^{-1}(q) \nabla_{z_q} \mathcal{H}_d \\ &\quad -\nabla_{z_p}^T \mathcal{H}_d \mathcal{B} \left( K_d - \frac{1}{2\sigma_a} K_a K_a^T \right) \mathcal{B}^T \nabla_{z_p} \mathcal{H}_d - \left( k_a - \frac{\sigma_a}{2} \right) x_a^T x_a \\ &\quad + \Sigma \mathcal{H} \left[ T_d + \sqrt{\lambda_{\max}(\mathcal{B}^T \mathcal{B})} u_{\max}^T u_{\max} (1 - \gamma) \right] \\ &\leq -\lambda \cdot \left( \|\nabla_{z_q} \mathcal{H}_d\|^2 + \|\nabla_{z_p} \mathcal{H}_d\|^2 + \|x_a\|^2 \right) + \sigma, \end{aligned}$$

where

$$\begin{aligned} \lambda &= \min \left\{ k_a - \frac{\sigma_a}{2}, \lambda_{\min} \left[ \mathcal{M}^{-1}(q) \mathcal{B} K_q \mathcal{B}^T \mathcal{M}^{-1}(q) \right], \right. \\ &\quad \left. \lambda_{\min} \left[ \mathcal{B} \left( K_d - \frac{1}{2\sigma_a} K_a K_a^T \right) \mathcal{B}^T \right] \right\} > 0, \\ \sigma &= \Sigma \mathcal{H} \left[ T_d + \sqrt{\lambda_{\max}(\mathcal{B}^T \mathcal{B})} u_{\max}^T u_{\max} (1 - \gamma) \right] \geq 0. \end{aligned}$$

Obviously, if  $\mathcal{M}^{-1}(q)$  is with bounded eigenvalues,  $\lambda$  would also be bounded.

Similar to the analysis shown in [15], above equation means if  $\|\nabla_{z_q} \mathcal{H}_d\|^2 + \|\nabla_{z_p} \mathcal{H}_d\|^2 + \|x_a\|^2 > \frac{\sigma}{\lambda}$ , there would be  $\dot{V}_{Ly_a} < 0$ , and the value of Lyapunov function would be decreased until  $\|\nabla_{z_q} \mathcal{H}_d\|^2 + \|\nabla_{z_p} \mathcal{H}_d\|^2 + \|x_a\|^2 \leq \frac{\sigma}{\lambda}$ . Consequently,  $\nabla_{z_q} \mathcal{H}_d$ ,  $\nabla_{z_p} \mathcal{H}_d$ , and  $x_a$  could ultimately converge to the definite sets with  $t \rightarrow +\infty$ , and these sets are also bounded with bounded  $\mathcal{M}^{-1}(q)$ .  $\square$

In this subsection, adaptive IDA-PBC is proposed and improved to deal with the loss of actuator effectiveness and actuator saturation. Based on some estimated parameters, the lower bound of actuator faults is not necessary for FTC design. An auxiliary state vector is introduced to guarantee the saturated control inputs could ensure the closed-loop stability. This vector actually allows the existence of actuator saturation in controller applications, and similar ideas are also proposed in [25] based on modified sector condition and quadratic polytopic differential inclusion. Compared with some references that avoid actuator saturation based on the intermediate control law [26] and segmented control inputs [27], the allowance of actuator saturation could make full use of the actuator capability to improve the closed-loop dynamic performance.

### 4 Simulation and Experiment Results

To validate the effectiveness of the proposed methods, the attitude control of a hexarotor UAV as shown in Fig. 1 will be considered in this section. The configuration of this UAV is shown in Fig. 2, where six rotors generate six

thrusts represented by  $f_i$  ( $i = 1, \dots, 6$ ),  $l$  means the distance from a rotor to center of gravity, and  $O_b X_b Y_b Z_b$  represents the body-axis coordinate system. The fault-free rotational dynamics of the hexarotor UAV could be represented as following PCH model:

$$\begin{bmatrix} \dot{q} \\ \dot{p} \end{bmatrix} = \begin{bmatrix} 0 & I_3 \\ -I_3 & 0 \end{bmatrix} \begin{bmatrix} \nabla_q \mathcal{H} \\ \nabla_p \mathcal{H} \end{bmatrix} + \begin{bmatrix} 0 \\ I_3 \end{bmatrix} \begin{bmatrix} M_x \\ M_y \\ M_z \end{bmatrix} + \begin{bmatrix} 0 \\ d \end{bmatrix}, \quad (28)$$

where  $q = [\phi \ \theta \ \psi]^T$  is the Euler angle vector,  $q_* = [\phi_* \ \theta_* \ \psi_*]^T$  would represent corresponding reference values,  $M_x$ ,  $M_y$ , and  $M_z$  are the moments in body-axis coordinate system generated by rotors and with control effects in different directions,  $\mathcal{H}(q, p) = \frac{1}{2} p^T \mathcal{M}^{-1}(q) p$  is the Hamiltonian function with only angular kinetic energy, and the inertia matrix is  $\mathcal{M}(q) =$

$$\mathcal{R}(q) \mathcal{J} \mathcal{R}^T(q) \text{ with } \mathcal{J} = \begin{bmatrix} I_{xx} & 0 & -I_{xz} \\ 0 & I_{yy} & 0 \\ -I_{xz} & 0 & I_{zz} \end{bmatrix} \text{ and } \mathcal{R}(q) = \begin{bmatrix} 1 & 0 & 0 \\ 0 & \cos \phi & -\sin \phi \\ -\sin \theta & \sin \phi \cos \theta & \cos \phi \cos \theta \end{bmatrix}.$$

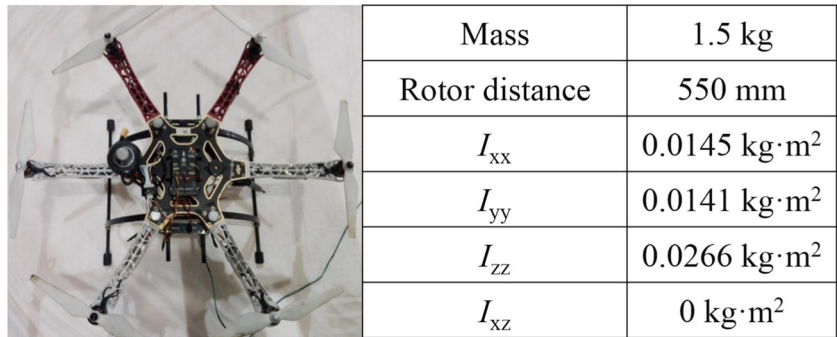
In following simulation results, the moments  $M_x$ ,  $M_y$ , and  $M_z$  would be regarded as control inputs, and attitude controllers would be designed for them by the proposed methods to track some step signals under different actuator faults.

For the attitude controller design in flight experiments, the forms of  $M_x$ ,  $M_y$ , and  $M_z$  should be considered further to deal with the uncertain actuator dynamics in the real platform. According to the configuration of the hexarotor UAV, the moments in (28) could be represented as follows [28]:

$$\begin{bmatrix} M_x \\ M_y \\ M_z \end{bmatrix} = \underbrace{\begin{bmatrix} -l & l & \frac{1}{2}l & -\frac{1}{2}l & -\frac{1}{2}l & \frac{1}{2}l \\ 0 & 0 & \frac{\sqrt{3}}{2}l & -\frac{\sqrt{3}}{2}l & \frac{\sqrt{3}}{2}l & -\frac{\sqrt{3}}{2}l \\ -c & c & -c & c & c & -c \end{bmatrix}}_{B_{\text{hex}}} \begin{bmatrix} u_1 - u_0 \\ u_2 - u_0 \\ u_3 - u_0 \\ u_4 - u_0 \\ u_5 - u_0 \\ u_6 - u_0 \end{bmatrix} \xi_f(t) \quad (29)$$

where  $c$  is a constant parameter for reaction torque,  $u_i$  ( $i = 1, \dots, 6$ ) is the control signal to generate thrust  $f_i$ ,  $\xi_f(t) > 0$  represents the actuator dynamics with  $f_i = \xi_f(t) \cdot u_i$ , and  $u_0 = \frac{1}{6} \sum_{i=1}^6 u_i$  with  $f_0 = \xi_f(t) \cdot u_0 =$

**Fig. 1** Hexarotor UAV platform and structure parameters [28]



$\frac{1}{6} \sum_{i=1}^6 f_i$ . For the hexarotor UAV,  $\xi_f(t)$  represents the aerodynamics of rotors and dynamics of driving motors, which is uncertain with varying battery voltage and flight maneuver. To simplify the attitude controller design with the actuator uncertainty, the following control signals are usually considered in real applications:

$$\begin{bmatrix} u_1 - u_0 \\ u_2 - u_0 \\ u_3 - u_0 \\ u_4 - u_0 \\ u_5 - u_0 \\ u_6 - u_0 \end{bmatrix} = \frac{1}{6} \underbrace{\begin{bmatrix} -2l^{-1} & 0 & -c^{-1} \\ 2l^{-1} & 0 & c^{-1} \\ l^{-1} & \frac{3}{\sqrt{3}}l^{-1} & -c^{-1} \\ -l^{-1} & -\frac{3}{\sqrt{3}}l^{-1} & c^{-1} \\ -l^{-1} & \frac{3}{\sqrt{3}}l^{-1} & c^{-1} \\ l^{-1} & -\frac{3}{\sqrt{3}}l^{-1} & -c^{-1} \end{bmatrix}}_{\mathcal{B}_{\text{hex}}^-} \begin{bmatrix} u_x \\ u_y \\ u_z \end{bmatrix}, \quad (30)$$

where  $\mathcal{B}_{\text{hex}}^-$  is the right inverse matrix of  $\mathcal{B}_{\text{hex}}$ ,  $u_x$ ,  $u_y$ , and  $u_z$  are three virtual control inputs, and  $u_0$  is the virtual control input for flight height control actually, which could be ignored directly in the attitude control. By introducing the above equation into (29), the following equivalent form of  $[M_x \ M_y \ M_z]^T$  could be formulated:

$$\begin{bmatrix} M_x \\ M_y \\ M_z \end{bmatrix} = \underbrace{\begin{bmatrix} \xi_x(t) & 0 & 0 \\ 0 & \xi_y(t) & 0 \\ 0 & 0 & \xi_z(t) \end{bmatrix}}_{\Xi(t)} \begin{bmatrix} u_x \\ u_y \\ u_z \end{bmatrix}. \quad (31)$$

In the ideal case, the diagonal elements of  $\Xi(t)$  are all equal to the uncertain actuator dynamics  $\xi_f(t)$ . However, due to the difference between actuators and assembly errors in the real platform, the uniform actuator uncertainties might not exist, so the subscripts x, y, and z are applied for the distinction between  $\xi_x(t)$ ,  $\xi_y(t)$ , and  $\xi_z(t)$ .

Based on the form of (31), the virtual control inputs  $u_x$ ,  $u_y$ , and  $u_z$  would be designed in following flight experiments, and (30) would be applied further to calculate the control signal of every actuator. Due to the actuator dynamics  $\Xi(t)$  in (31) is uncertain with varying battery voltage and flight maneuver, the diagonal elements  $\xi_\star(t)$  ( $\star = x, y, \text{ and } z$ ) are difficult to estimate accurately. However, if its upper bound  $\bar{\xi}_\star$  is known, it would be easy

to reformulate the uncertain actuator dynamics as  $\xi_\star(t) = \bar{\xi}_\star \gamma_\star(t)$ , where  $0 < \gamma_\star(t) \leq 1$ . Consequently, uncertain matrix  $\Xi(t)$  could be transformed into the actuator fault formulation as

$$\underbrace{\begin{bmatrix} \xi_x(t) & 0 & 0 \\ 0 & \xi_y(t) & 0 \\ 0 & 0 & \xi_z(t) \end{bmatrix}}_{\Xi(t)} = \underbrace{\begin{bmatrix} \bar{\xi}_x & 0 & 0 \\ 0 & \bar{\xi}_y & 0 \\ 0 & 0 & \bar{\xi}_z \end{bmatrix}}_{\mathcal{B}} \underbrace{\begin{bmatrix} \gamma_x(t) & 0 & 0 \\ 0 & \gamma_y(t) & 0 \\ 0 & 0 & \gamma_z(t) \end{bmatrix}}_{\Gamma(t)}, \quad (32)$$

where  $\Gamma(t)$  is within the bounded range  $0 < \gamma I_3 \leq \Gamma(t) \leq I_3$ , and  $\gamma = \xi_\star / \bar{\xi}_\star$  with  $\bar{\xi}_\star$  as the lower bound of  $\xi_\star(t)$ . To deal with the actuator uncertainty with the fault formulation (32), the diagonal elements in  $\Xi(t)$  would be estimated offline by UKF in following contents, and the values of  $\mathcal{B}$  and  $\gamma$  would be determined based on the upper and lower bounds of estimations. Then high-gain IDA-PBC would be designed for the rolling stability of the UAV in hovering flight experiments under the actuator uncertainty and further actuator fault.

To achieve the hovering flight in following experiments, the necessary position control as well as pitching and yawing stability would be achieved based on the typical RUAV control method proposed in [29]. Moreover, the actuator fault for the virtual control input  $u_x$  about rolling

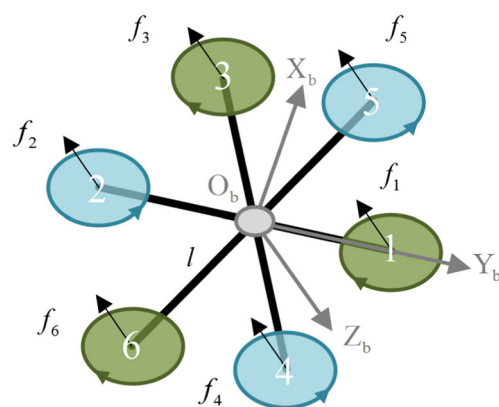


**Fig. 2** Configuration of the hexarotor UAV platform

**Table 1** Controllers and parameters for four simulation cases

No.	Controller	Parameters	Note
Case 1	General IDA-PBC from (3)	$\mathcal{M}_d = \mathcal{J}, \mathcal{V}_d = \frac{1}{2}(p - p_*)^T K_p (p - p_*), K_p = 4\mathcal{J}, K_d = \text{diag}(0.02, 0.02, 0.02), K_q = \text{diag}(0.02, 0.02, 0.02)$	No fault
Case 2	High-gain IDA-PBC from Theorem 1	$\mathcal{M}_d = \mathcal{J}, K_p = 4\mathcal{J}, M_1 = \text{diag}(0.02, 0.02, 0.02), M_2 = \text{diag}(0.02, 0.02, 0.02), \sigma_1, \sigma_2,$ and $\sigma_3$ are from (19), $K_d = 1.01 \left[ \frac{\sigma_1 + \sigma_2 + \sigma_3}{2\gamma} \cdot (1 - \gamma)^2 I_3 + \frac{M_1}{\gamma} \right], K_q = M_2$	With fault
Case 3			With fault
Case 4	Adaptive IDA-PBC from Corollary 1	$\mathcal{M}_d = \mathcal{J}, \mathcal{V}_d = \frac{1}{2}(p - p_*)^T K_p (p - p_*), K_p = 4\mathcal{J}, K_d = \text{diag}(0.02, 0.02, 0.02), K_q = \text{diag}(0.02, 0.02, 0.02), K_a = \text{diag}(0.001, 0.001, 0.001), k_a = k_d = k_\gamma = 0.1, \Sigma_{\mathcal{H}} = 0.05, \sigma_a = 0.99 \cdot 2k_a$	With fault

dynamics would be introduced further by software in following flight experiments. The fault for the virtual control input usually means simultaneous faults of several actual actuators, which might be infrequent in real platforms. However, this faulty case is convenient to validate the applied control method, which focuses on virtual control inputs based on (31). Note that, according to the form of (29),  $\mathcal{B}_{\text{hex}}$  is a row full rank matrix with the right inverse matrix  $\mathcal{B}_{\text{hex}}^-$  shown in (30), so the proposed methods in this paper could deal with the faults

on actual actuators of the hexarotor UAV absolutely. Due to the configurations of hexarotor UAVs provide redundant actuators for fault-tolerance [30, 31], the quadrotor UAV might be more suitable than hexarotor UAV for the control performance validation under the faults on actual actuators. The faulty case for the virtual control input is also an expedient strategy to avoid the fault-tolerant ability from the UAV configuration. After all, the main purpose of flight experiments is to validate the proposed FTC method by a real platform.

**Fig. 3** Euler angles with different controllers (zooms show some details of curves)

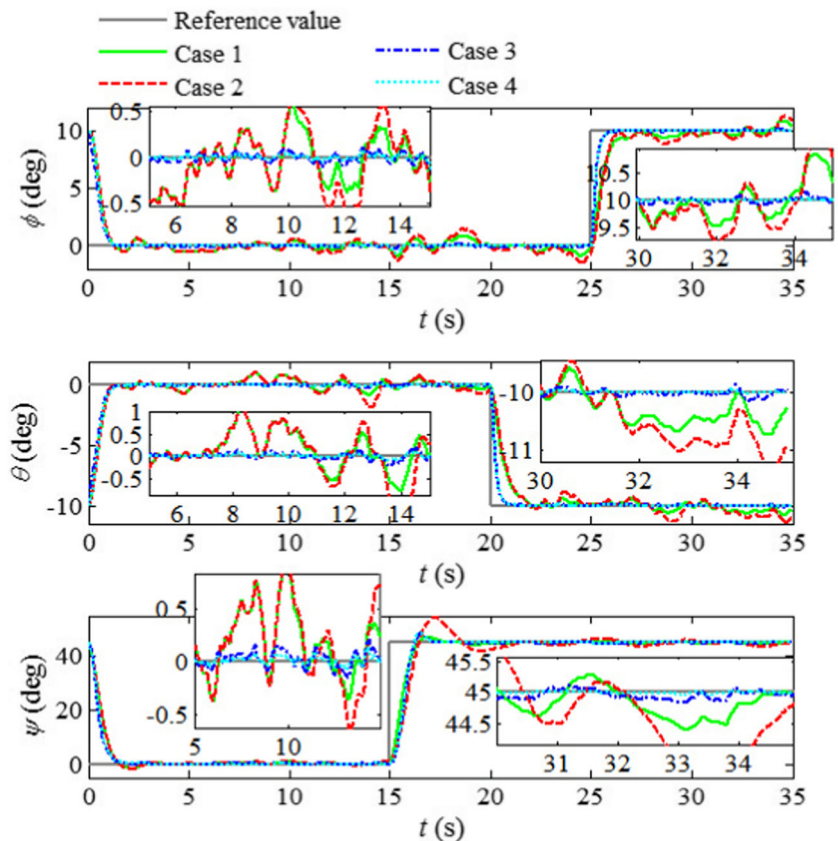
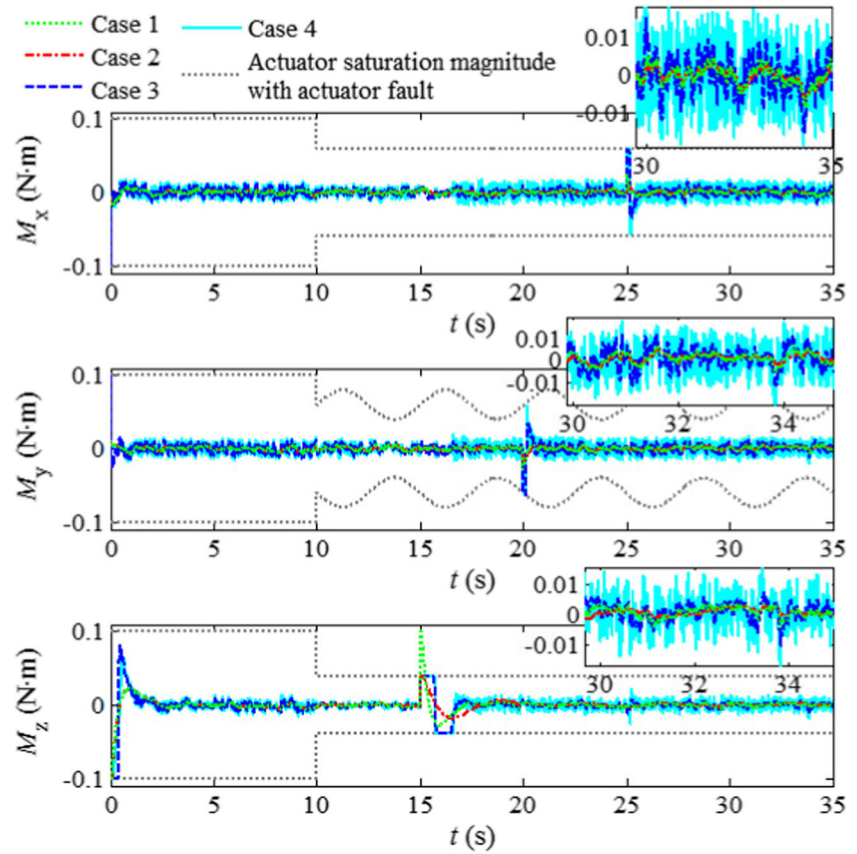


**Fig. 4** Control inputs from different controllers (zooms show some details of curves)



**4.1 Simulation Results**

To compare with different control methods in four simulation cases, the applied controllers and parameters are listed in Table 1, where Case 1 and Case 2 apply same controller, but no fault is introduced into Case 1. For Case 2~4, following actuator faults are considered:

$$\gamma_x(t) = \begin{cases} 1, & t \leq 10s \\ 0.6, & t > 10s \end{cases}, \gamma_z(t) = \begin{cases} 1, & t \leq 10s \\ 0.4, & t > 10s \end{cases}$$

$$\gamma_y(t) = \begin{cases} 1, & t \leq 10s \\ 0.6 + 0.2 \sin(0.4\pi t), & t > 10s \end{cases}$$

According to above equations, the lower bound of actuator faults for Case 3 is  $\gamma = 0.4$ . Note that, to present the results within finite simulation time, the actuator faults are set up to occur synchronously, but the proposed methods could deal with the varying faults that occur at different time points.

For following simulation results, the initial Euler angles and their final reference values are set as  $[10^\circ \ -10^\circ \ 45]^\top$ , the time-varying disturbances are all uniformly distributed

**Table 2** Criterion for simulation results in four cases<sup>†</sup>

		ave(●)	std(●)	ave(●)	std(●)	ave(●)	std(●)
		$ \phi_* - \phi $		$ \theta_* - \theta $		$ \psi_* - \psi $	
Case 1	5~10s	0.237	0.157	0.333	0.342	0.353	0.248
	10~15s	0.210	0.139	0.328	0.218	0.227	0.202
Case 2	5~10s	0.237	0.157	0.333	0.342	0.353	0.248
	10~15s	0.331	0.191	0.563	0.481	0.342	0.246
Case 3	5~10s	0.033	0.019	0.037	0.033	0.061	0.041
	10~15s	0.042	0.027	0.074	0.056	0.071	0.044
Case 4	5~10s	0.014	0.009	0.017	0.015	0.028	0.019
	10~15s	0.021	0.014	0.035	0.027	0.037	0.025

<sup>†</sup> All criterion are with unit deg



random signals between  $-0.1$  and  $0.1$ , and the control inputs are limited within  $[-0.1, 0.1]$ . Although general IDA-PBC and high-gain IDA-PBC from Theorem 1 do not consider the actuator saturation, saturation blocks are applied artificially for same simulation conditions with adaptive IDA-PBC from Corollary 1. The curves of Euler angles and control inputs are displayed in Figs. 3 and 4, where the magnitudes of  $M_x$ ,  $M_y$ , and  $M_z$  increase at 25s, 20s, and 15s to track the reference values of  $\phi$ ,  $\theta$ , and  $\psi$ . Note that the actuator faults reduce the actuator saturation magnitudes as shown in Fig. 4 due to the form of  $\Gamma\text{sat}(v)$  in the controlled plant (8) and (9), which is consistent with the real applications as previous discussion.

Table 2 further lists the averages and standard derivations of absolute tracking errors in different simulation periods, where  $\text{ave}(\bullet)$  and  $\text{std}(\bullet)$  represent average and standard derivation operators. For a discrete-time signal  $\mathcal{X}(kT)$  ( $t = kT$ ) with  $k$  and  $T$  as sampling number and period,  $\text{ave}(\mathcal{X}(kT)) = \frac{1}{N} \sum_{i=1}^N X(iT)$  and  $\text{std}(\mathcal{X}(kT)) = \sqrt{\frac{1}{N} \sum_{i=1}^N [X(iT) - \text{ave}(\mathcal{X}(kT))]^2}$  in  $N$  sampling periods. Obviously, after actuator faults (occur at 10s), the control performance of the general IDA-PBC in Case 2 degenerates, and more vibrations of states appear as shown in Fig. 3. Due to inherently excellent control performance, high-gain IDA-PBC in Case 3 and adaptive IDA-PBC in Case 4 still keep good control performance after actuator faults. According to Fig. 4, the control inputs  $M_x$ ,  $M_y$ , and  $M_z$  of Case 3 and Case 4 are with more fluctuations than Case 1 and Case 2 for good control performance. Relatively speaking, adaptive

IDA-PBC is with better disturbance attenuation than high-gain IDA-PBC, and corresponding control inputs fluctuate more dramatically as show in Fig. 4. If reduce the value of  $\Sigma_{\mathcal{H}}$ , the disturbance attention of adaptive IDA-PBC would be much better, but the fluctuations of control inputs would also be severer.

### 4.2 Experiment Results

Flight experiments mainly validate high-gain IDA-PBC. To transform the uncertain actuator dynamics of the real platform into the actuator fault formulation (32), the diagonal elements of matrix  $\Xi$  should be estimated. Similar to the modeling of actuator faults in [32], the derivatives of  $\xi_x$ ,  $\xi_y$ , and  $\xi_z$  could also be assumed as stationary random processes. Based on the Newton-Euler equation about attitude dynamics,  $\xi_x$ ,  $\xi_y$ , and  $\xi_z$  could be estimated jointly with angular velocities  $[\omega_x \ \omega_y \ \omega_z]^T$  by UKF, and the fault-free flight data including hovering and regular attitude variations are applied for these estimations. Detailed contents about UKF design could refer to [22] and [32], and are ignored here. To apply high-gain IDA-PBC for rolling motion control, Fig. 5 displays the offline estimations about  $\omega_x$  and  $\xi_x$ . With these results, the upper and lower bounds of  $\xi_x$  could be chosen as  $\bar{\xi}_x = 7.1$  and  $\underline{\xi}_x = 1.6$ . Consequently, constant  $\mathcal{B}$  and the lower bound of  $\gamma_x$  for the actuator fault formulation (32) are determined as 7.1 and  $1.6/7.1 \approx 0.225$  for rolling dynamics.

By assuming that other degree-of-freedoms have been stabilized, the controller for rolling motion could be designed as follows according to (13) with  $\mathcal{M}(q) = \mathcal{M}_d = I_{xx}$ ,  $q = \phi$ , and  $q_* = \phi_*$ :

$$u_x = \left( \mathcal{B}^{-1} K_p + K_{dB}^T I_{xx}^{-1} \mathcal{B} K_q \mathcal{B}^T I_{xx}^{-1} K_p \right) (\phi_* - \phi) - \left( K_{dB}^T + K_q \mathcal{B}^T I_{xx}^{-1} K_p \right) \dot{\phi}.$$

According to (14) and (15), following inequalities should be satisfied:

$$\sigma_1 \geq \frac{(K_q \mathcal{B}^T I_{xx}^{-1} K_p \mathcal{B}^T)^2}{2M_1} > 0, \quad \sigma_2 \geq \frac{(\mathcal{B}^{-1} I_{xx})^2}{M_2} > 0,$$

$$\sigma_3 \geq \frac{(K_q \mathcal{B}^T I_{xx}^{-1} K_p I_{xx}^{-1} \mathcal{B} K_q \mathcal{B}^T)^2}{M_2} > 0,$$

$$\gamma K_d > \frac{\sigma_1 + \sigma_2 + \sigma_3}{2} (1 - \gamma)^2 + M_1, \quad \mathcal{B} K_q \mathcal{B}^T \geq M_2.$$

For high-gain IDA-PBC under only actuator uncertainty, the value of  $\gamma$  is set as  $1.6/7.1 \approx 0.225$ ; to consider the loss of actuator effectiveness not more than 40% (occur at around 77.5s), the value is set as  $\gamma = 1.6/7.1 \cdot 0.6 \approx 0.135$  for the controller under actuator uncertainty and fault. Other parameters in above controller are set as:  $M_1 = M_2 =$

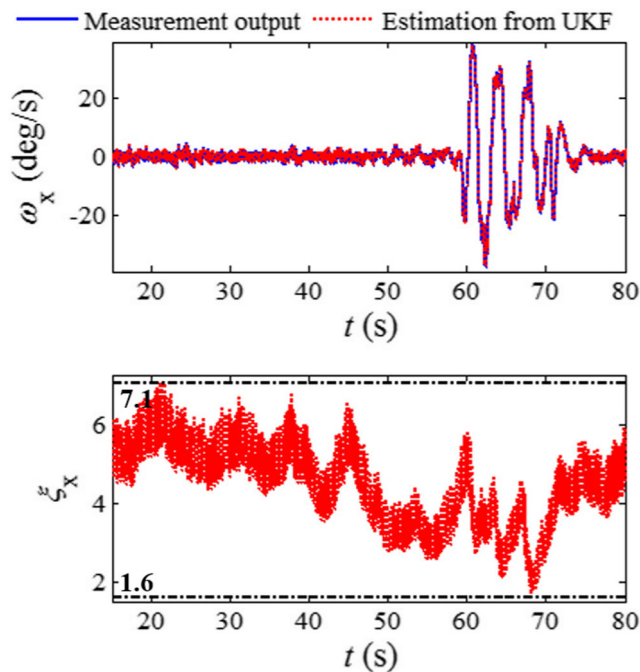
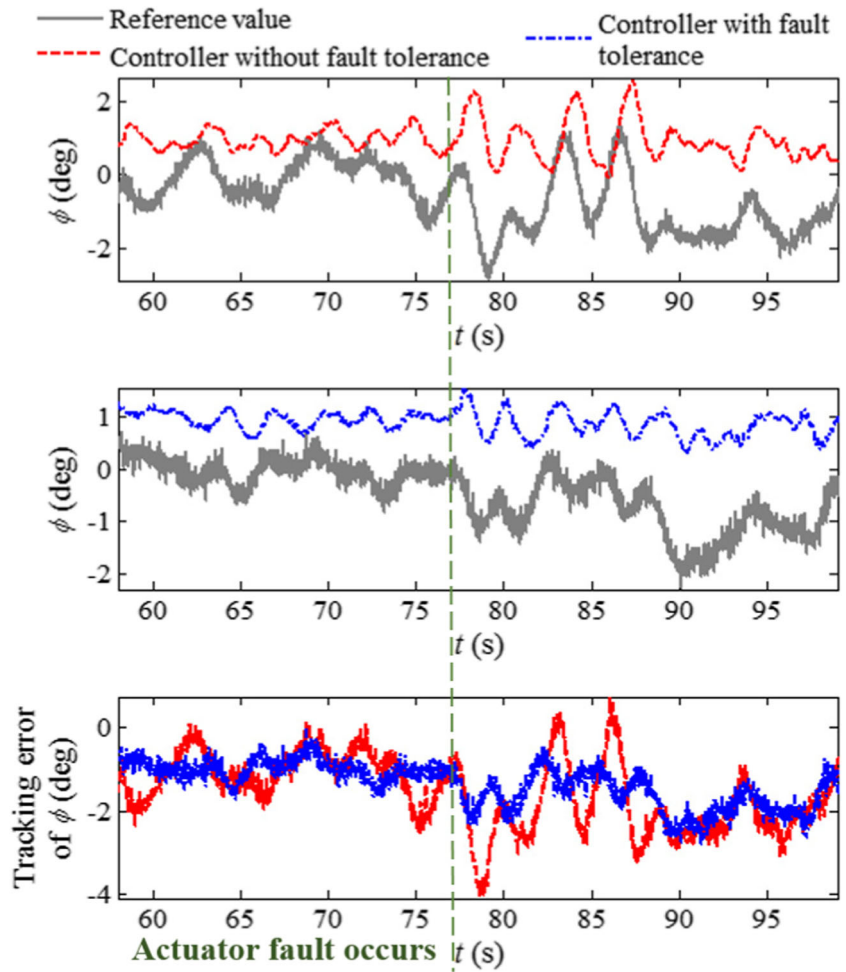
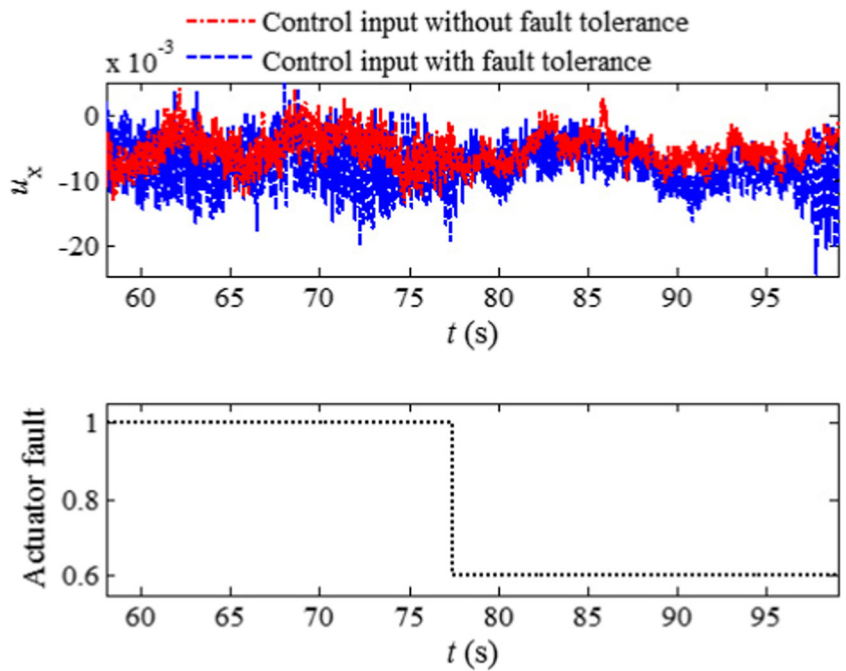


Fig. 5 UKF estimation results

**Fig. 6**  $\phi$  and tracking error with different controllers in hovering flight experiments



**Fig. 7**  $u_x$  from different controllers and actuator fault





**Table 3** Criterion in flight experiments with High-gain IDA-PBC<sup>†</sup>

	ave(  $\phi_*$ - $\phi$  )		std(  $\phi_*$ - $\phi$  )	
	Fault-free	Faulty	Fault-free	Faulty
Without fault- tolerance ( $\gamma \approx 0.225$ )	1.074	1.987	0.532	0.835
With fault- tolerance ( $\gamma \approx 0.135$ )	0.976	1.675	0.250	0.471

<sup>†</sup>All criterion are with unit deg

0.003,  $K_p = 10I_{xx}$ ,  $K_d = 1.01 \left[ \frac{\sigma_1 + \sigma_2 + \sigma_3}{2\gamma} (1 - \gamma)^2 + \frac{M_1}{\gamma} \right]$ , and  $K_q = B^{-1} M_2 B^T$ .

The curves of attitude information and control inputs in the hovering flight experiments are displayed in Figs. 6 and 7, where the reference value of  $\phi$  is generated for the position control based on the method in [29]. Moreover, Table 3 lists the averages and standard derivations of absolute tracking errors. After the actuator fault, the control performance of the controller without fault-tolerance degenerates obviously. The proposed high-gain controller with fault-tolerance owns better disturbance attenuation. Above all, it could ensured the closed-loop stability under actuator faults based on passivity. The advantages of the proposed controller would be more obvious, if a severer actuator fault is introduced. For safe flight experiments, only a nonlethal fault (loss of actuator effectiveness not more than 40%) is considered here. Moreover, together with better disturbance attenuation, the control inputs with fault-tolerance also accompany with more dramatic fluctuations similar to the results from simulation.

### 5 Conclusion

This paper focuses on the FTC based on IDA-PBC. High-gain and adaptive IDA-PBC methods are proposed under loss of actuator effectiveness. Although the loss of actuator effectiveness with specific lower bound is not fatal, the control performance under it degenerates obviously. The proposed high-gain and adaptive IDA-PBC methods could still keep the control performance and good disturbance attention under actuator faults. The faulty case with actuator saturation and unknown lower bound of actuator faults is dealt with further in adaptive IDA-PBC method. Some simulation results are displayed to illustrate the control effectiveness. Moreover, the uncertain actuator dynamics of the real platform is transformed into the actuator fault formulation, and high-gain IDA-PBC is applied for hovering flight experiments under the actuator uncertainty and further actuator fault.

**Acknowledgements** This work was supported by National Key Research and Development Program of China (No. 2017YFD0701002) and National Natural Science Foundation of China (Nos. 91748130 and U1608253).

### References

- Ortega, R., Loria, A., Nicklasson, P.J., Sira-Ramirez, H.: *Passivity-based Control of Euler-Lagrange Systems*. Springer, UK (1998)
- Ortega, R., Schaft, A., Maschke, B., Escobar, G.: Interconnection and damping assignment passivity-based control of port-controlled Hamiltonian systems. *Automatica* **38**(4), 585–596 (2002)
- Ortega, R., Spong, M.W., Gomez-Estern, F., Blankenstein, G.: Stabilization of a class of underactuated mechanical systems via interconnection and damping assignment. *IEEE T. Automat. Contr.* **47**(8), 1218–1233 (2002)
- Acosta, J.A., Sanchez, M.I., Ollero, A.: Robust control of underactuated aerial manipulators via IDA-PBC. In: *53rd IEEE Conference on Decision and Control*, pp 673–678. Los Angeles, USA (2014)
- Bouid, Y., Siguerdidjane, H., Bestaoui, Y., Zareb, M.: Energy based 3D autopilot for VTOL UAV under guidance & navigation constraints. *J. Intell. Robot. Syst.* **87**(2), 341–362 (2017)
- Guerrero-Sanchez, M.E., Mercado-Ravell, A., Lozano, R., Garcia-Beltran, C.D.: Swing-attenuation for a quadrotor transporting a cable-suspended payload. *ISA Trans.* **68**, 433–449 (2017)
- Serra, F.M., Angelo, C.H.D., Forchetti, D.G.: IDA-PBC Control of a DC-AC converter for sinusoidal three-phase voltage generation. *Int. J. Electron.* **104**(1), 93–110 (2016)
- Zhang, Y., Jiang, J.: Bibliographical review on reconfigurable fault-tolerant control systems. *Annu. Rev. Control* **32**(2), 229–252 (2008)
- Nasiri, A., Nguang, S.K., Swain, A., Almahles, D.: Passive actuator fault tolerant control for a class of MIMO nonlinear systems with uncertainties. *Int. J. Control* **92**(3), 693–704 (2019)
- Shen, Q., Wang, D., Zhu, S., Poh, E.K.: Integral-type sliding mode fault-tolerant control for attitude stabilization of spacecraft. *IEEE T. Contr. Syst. T.* **23**(3), 1131–1138 (2015)
- Wang, B., Zhang, Y.: An adaptive fault-tolerant sliding mode control allocation scheme for multirotor helicopter subject to simultaneous actuator faults. *IEEE T. Ind. Electron.* **65**(5), 4227–4236 (2018)
- Li, Y., Yang, G.: Adaptive asymptotic tracking control of uncertain nonlinear systems with input quantization and actuator faults. *Automatic* **72**, 177–185 (2016)
- Xiao, B., Hu, Q., Friswell, M.I.: Active fault-tolerant attitude control for flexible spacecraft with loss of actuator effectiveness. *Int. J. Adapt. Control* **27**(11), 925–943 (2013)
- Lin, X., Dong, H.: Tuning function-based adaptive backstepping fault-tolerant control for nonlinear systems with actuator faults and multiple disturbances. *Nonlinear Dynam.* **91**(4), 2227–2239 (2018)
- Hu, Q., Xiao, B.: Fault-tolerant attitude control for spacecraft under loss of actuator effectiveness. *J. Guid. Control Dynam.* **34**(3), 927–932 (2011)
- Lopez-Estrada, F.R., Ponsart, J., Theilliol, D., Zhang, Y., Astorga-Zaragoza, C.: LPV Model-based tracking control and robust sensor fault diagnosis for a quadrotor UAV. *J. Intell. Robot. Syst.* **84**(1-4), 163–177 (2016)

17. Liu, Z., Theilliol, D., Yang, L., He, Y., Han, J.: Observer-based linear parameter varying control design with unmeasurable varying parameters under sensor faults for quad-tilt rotor unmanned aerial vehicle. *Aerosp. Sci. Technol.* **92**, 696–171 (2019)
18. Chen, J., Zhang, W., Cao, Y., Chu, H.: Observer-based consensus control against actuator faults for linear parameter-varying multiagent systems. *IEEE T. Syst. Man Cy.-S.* **47**(7), 1336–1347 (2017)
19. Jiang, J., Yu, X.: Fault-tolerant control systems: a comparative study between active and passive approaches. *Annu. Rev. Control* **36**(1), 60–72 (2012)
20. Benosman, M., Lum, K.Y.: Application of passivity and cascade structure to robust control against loss of actuator effectiveness. *Int. J. Robust Nonlin.* **20**(6), 673–693 (2010)
21. Donaire, A., Romero, J.G., Ortega, R., Siciliano, B., Crespo, M.: Robust IDA-PBC for underactuated mechanical systems subject to matched disturbances. *Int. J. Robust Nonlin.* **27**(6), 1000–1016 (2017)
22. Wan, E.A., Merwe, R.: The unscented kalman filter for nonlinear estimation. In: *IEEE 2000 Adaptive Systems for Signal Processing, Communications, and Control Symposium*, pp. 1–6. Alberta, Canada (2000)
23. Zhang, X., Zhang, Y., Su, C., Feng, Y.: Fault-tolerant control for quadrotor UAV via backstepping approach. In: *48Th AIAA Aerospace Sciences Meeting including the New Horizons Forum and Aerospace Exposition*, pp. 1–12. Florida, USA (2010)
24. Khalil, H.K. *Nonlinear Systems*, 2nd edn. Prentice Hall, USA (2002)
25. Hashemi, M., Egoli, A.K., Naraghi, M.: Integrated fault tolerant control for saturated systems with additive faults: a comparative study of saturation models. *Int. J. Control Autom.* **17**(4), 1019–1030 (2019)
26. Shao, X., Hu, Q., Shi, Y., Jiang, B.: Fault-tolerant prescribed performance attitude tracking control for spacecraft under input saturation. *IEEE T. Contr Syst. T.*, pp. 1–9 (2018)
27. Shen, Q., Yue, C., Goh, C.H., Wang, D.: Active fault-tolerant control system design for spacecraft attitude maneuvers with actuator saturation and faults. *IEEE T. Ind. Electron.* **22**(6), 3763–3772 (2019)
28. Dai, B., He, Y., Zhang, G., Gu, F., Yang, L., Xu, W.: Wind disturbance rejection for unmanned aerial vehicle based on acceleration feedback method. In: *IEEE 2018 Conference on Decision and Control*, pp. 4680–4686. Miami Beach, USA (2018)
29. Lee, T., Leok, M., McClamroch, H.: Nonlinear robust tracking control of a quadrotor UAV on SE(3). *Asian J. Control* **15**(3), 1–18 (2013)
30. Schneider, T., Ducard, G., Rudin, K., Strupler, P.: Faulttolerant control allocation for multirotor helicopters using parametric programming. In: *International Micro Air Vehicle Confrence and Flight Competition*. Braunschweig, Germany (2012)
31. Du, G., Quan, Q., Cai, K.: Controllability analysis and degraded control for a class of hexacopters subject to rotor failures. *J. Intell. Robot. Syst.* **78**(1), 143–157 (2015)
32. Qi, J., Song, D., Wu, C., Han, J., Wang, T.: KF-Based adaptive UKF algorithm and its application for rotorcraft UAV actuator failure estimation. *Int. J. Adv. Robot. Syst.* **9**(4), 1–9 (2012)

**Publisher's Note** Springer Nature remains neutral with regard to jurisdictional claims in published maps and institutional affiliations.

**Zhong Liu** was born in Jining, China, in 1991. He received the B.S. degree in automation from Shandong University, Weihai, China, in 2014. He is currently working towards Ph.D. degree in pattern recognition and intelligent system at Shenyang Institute of Automation, Chinese Academy of Sciences, Shenyang, China, Institutes for Robotics and Intelligent Manufacturing, Chinese Academy of Sciences, Shenyang, China, and University of the Chinese Academy of Sciences, Beijing, China.

His main research interests include nonlinear modeling, nonlinear control of unmanned aerial vehicles, and linear parameter-varying control.

**Didier Theilliol** received the Ph.D. degree in control engineering from Nancy University, Vandoeuvre- Les-Nancy, France, in 1993.

He currently is a Full Professor in Research Center of Automatic Control of Nancy at University of Lorraine, France. He coordinates and leads national, European, and international research and development projects in steel industries, wastewater treatment plant, or aerospace domain. His current research interests include intelligent and classical model-based fault diagnosis method synthesis, active fault-tolerant control system design for linear time invariant, linear parameter varying, and multi-linear systems and also reliability analysis. Didier Theilliol was the General Chair and Program Chair of various international conference sponsored by IEEE and IFAC. He is a leader chair of a novel Conference on Control and Fault-Tolerant Systems (co-sponsored IEEE CSS and IEEE CS) dedicated to review the current activities in the field of Advanced Control and Diagnosis and their implication in Maintenance (Nice, 2010, 2013, 2016 and 2019). He is currently an Associate Editor of *ISA Transactions Journal*, *International Journal of Applied Mathematics & Computer Science* and *Journal of Intelligent and Robotic Systems*. Didier Theilliol was Associate Editor of *IEEE Transactions on Reliability* (2013-2016) and of *Unmanned Systems journal* (2012-2017).

**Liyang Yang** was born in Taiyuan, China, in 1979. She received the B.S. degree and master degree from Shenyang Jianzhu University, Shenyang, China, in 2002 and 2005, and the Ph.D. degree from Shenyang Institute of Automation, Chinese Academy of Sciences, Shenyang, China, in 2011.

She is currently a Associate Professor of State Key Laboratory of Robotics, Shenyang Institute of Automation, Chinese Academy of Sciences, Shenyang, China, and Institutes for Robotics and Intelligent Manufacturing, Chinese Academy of Sciences, Shenyang, China. Her main research interests include nonlinear control and autonomous robot planning.


**Yuqing He** was born in Weihui, China, in 1980. He received the B.S. degree in engineering and automation from Northeastern University, Qinhuangdao, China, in 2002, and the Ph.D. degree from Shenyang Institute of Automation, Chinese Academy of Sciences, Shenyang, China, in 2008.

He is currently a Professor of State Key Laboratory of Robotics, Shenyang Institute of Automation, Chinese Academy of Sciences, Shenyang, China, and Institutes for Robotics and Intelligent Manufacturing, Chinese Academy of Sciences, Shenyang, China. In 2012, he was a Visiting Researcher at the Institute for Automatic Control Theory, Technical University of Dresden, Germany. His main research interests include nonlinear estimation, control, and cooperation of multiple robots.

**Jianda Han** was born in Liaoning, China, in 1968. He received the Ph.D. degree from Harbin Institute of Technology, Harbin, China, in 1998.

He is currently a Professor of Institute of Robotics and Automatic Information Systems, College of Artificial Intelligence, and Tianjin Key Laboratory of Intelligent Robotics, Nankai University, Tianjin, China, State Key Laboratory of Robotics, Shenyang Institute of Automation, Chinese Academy of Sciences, Shenyang, China, and Institutes for Robotics and Intelligent Manufacturing, Chinese Academy of Sciences, Shenyang, China. His research interests include nonlinear estimation and control, robotics, and mechatronics systems.

## Affiliations

Zhong Liu<sup>1,2,3</sup> · Didier Theilliol<sup>4</sup>  · Liying Yang<sup>1,2</sup> · Yuqing He<sup>1,2</sup> · Jianda Han<sup>1,2,5,6</sup>

Zhong Liu  
liuzhong@sia.cn

Liying Yang  
yangliying@sia.cn

Yuqing He  
heyuqing@sia.cn

Jianda Han  
jdhan@sia.cn

- <sup>1</sup> State Key Laboratory of Robotics, Shenyang Institute of Automation, Chinese Academy of Sciences, 110016, Shenyang, Liaoning Province, People's Republic of China
- <sup>2</sup> Institutes for Robotics and Intelligent Manufacturing, Chinese Academy of Sciences, 110169, Shenyang, Liaoning Province, People's Republic of China
- <sup>3</sup> University of Chinese Academy of Sciences, 100049, Beijing, People's Republic of China
- <sup>4</sup> CRAN UMR 7039, CNRS, University of Lorraine, Faculte des Sciences et Techniques, B.P. 70239, 54506, Vandœuvre-Lés-Nancy, France
- <sup>5</sup> Institute of Robotics and Automatic Information Systems, College of Artificial Intelligence, Nankai University, Tianjin, People's Republic of China
- <sup>6</sup> Tianjin Key Laboratory of Intelligent Robotics, Nankai University, 300350, Tianjin, People's Republic of China